Electrical Power and Energy Systems 149 (2023) 109050

Contents lists available at ScienceDirect

International Journal of Electrical Power and Energy Systems

journal homepage: www.elsevier.com/locate/ijepes

Experimental validation of a novel power smoothing method for on-grid photovoltaic systems using supercapacitors

Darío Benavides [a,b], Paul Arévalo [b,c], José A. Aguado [a], Francisco Jurado [c,*]

[a] Department of Electrical Engineering, University of Málaga, 29010 Málaga, Spain
[b] Department of Electrical, Electronics and Telecommunications Engineering, University of Cuenca, 010107 Cuenca, Ecuador
[c] Department of Electrical Engineering, University of Jaen, 23700 Jaén, Spain

ARTICLE INFO

Keywords:
Predictor corrector
Power smoothing
Supercapacitor
photovoltaic power generation
State of charge

ABSTRACT

Renewable energy sources have been widely developed in grid-connected systems. However, a challenge to overcome is the random characteristic of renewable resources such as solar irradiance, photovoltaic power fluctuations caused by cloud movement could cause instability of the utility grid. To solve this drawback, several authors have proposed various power smoothing methods for photovoltaic systems using supercapacitors. Nevertheless, sizing optimization and operability of the supercapacitor has not been properly studied. Forecasting power fluctuations is an important strategy to avoid the unnecessary operation of the supercapacitor in certain cases. In this paper, a novel power smoothing method (predictor – corrector) using supercapacitors for a grid-connected photovoltaic system is proposed, the method consists of two stages, prediction and correction. The main novelty of the new method is the use a simple k-means algorithm application model in the cycle estimation stage for supercapacitors, with the aim of selecting representative data of power fluctuations and supercapacitor charge/discharge cycles. Then, for the correction stage, the novel proposed method uses ramp rate algorithms to generate the reference signal to control the state of charge of the supercapacitor.

The validation of the new proposed method has been done through exhaustive laboratory experiments under different cloudiness events. The results show that the energy losses when applying the new method are lower with respect to the moving average and ramp rate methods. Furthermore, the number of technical violations is reduced, demonstrating the feasibility of the proposed method to ensure successful mitigation of PV power fluctuations.

1. Introduction

Renewable power generation sources such as photovoltaics (PV) have received considerable attention around the world. However, due to the movement of the clouds, the PV energy production is highly random which cause instability in the utility grid [1], causing voltage fluctuations, reverse power flow, involuntary absenteeism, power peaks and frequency variations [2], being necessary leveling the intermittent sources output to maintain grid stability [3] and avoid reducing the power quality by generating harmonic voltages in the grid and reliability problems [4]. Frequently, the hybridization of batteries storage systems (BSS) and supercapacitors (SC) is the combination used to reduce the power fluctuations of a renewable energy system (RES) [5], where the authors mention the reduction of the performance and lifespan of the BSS when subjected to different regimes of operation [6], the BSS technologies most commonly used in power smoothing techniques are lead acid and lithium ion [7]. The impact of power smoothing techniques on the long-term performance of BSS is studied in [8], where the authors indicate that BSS need to be replaced several times throughout the lifetime of the PV. Besides, including a hybrid energy storage system (HESS) to reduce the power fluctuations of RES, the capital cost increases considerably, the authors in [9] indicate the impact of power smoothing techniques on performance in the long-term analysis of BSS, the authors present an accurate model of BSS based on the "rainflow cycle counting" algorithm to estimate the aging cycle of BSS, the results indicate that the application of BSS to reduce power fluctuations represents its decrease in average life expectancy, it is important to mention that the authors in Ref. [9] do not present a detailed study or classification of power fluctuations. On the other hand, sizing optimization of HESS to smooth power peaks is studied in [9], the

* Corresponding author.
E-mail address: fjurado@ujaen.es (F. Jurado).

https://doi.org/10.1016/j.ijepes.2023.109050
Received 5 October 2022; Received in revised form 4 February 2023; Accepted 19 February 2023
Available online 7 March 2023

proposed method is based on discrete wavelet transform and is solved by the weighted linear method and Benders decomposition, computer simulations show that the proposed scheme is capable of lowering charge/discharge current levels in BSS. However, the authors do not consider the computational effort of the method, which could cause a significant increase in the operating cost for a residential system and it has not been validated experimentally either. In this sense, in Ref. [10] a new approach for the control of the ramp rate (RR) of a PV system using BESS has been proposed, despite having done experimental validations to demonstrate the feasibility of the new method proposed, the forecasting of power fluctuations that could complement the new method that uses real-time data to reduce fluctuations is not considered, computational effort is another gap in the study. The literature mentions the advantage of using SC in intermittent energy systems due to its high power density [10]. The fast response of the SC allows to control the PV power output in short time steps, where various innovative methods of power smoothing have been developed from the technical and economic viewpoint [11]. Nevertheless, the random characteristic of the power fluctuations could cause a wrong operating of the SC maintaining unnecessary charge levels, forecasting power fluctuations could optimize SC operation, a topic that has been poorly studied in the literature and needs further investigation. Forecasting data is a study that allows knowing the future behavior of certain values to planning an electrical system with greater precision, in Ref. [12] the authors use high-resolution environmental data using annual estimates of power generation and RR for a reference PV site, the results show that varying design parameters from a typical "optimum" power configuration can reduce RR by nearly 50%, in this case, a computational optimization study of prediction methods with several high-resolution input variables would be promising.

Until now, in the literature review the effects of partial shading on PV are well known and have been extensively studied in recent years. Several authors propose methods to reduce power fluctuations, e.g., the Ref. [6] presents a comparative study of RR control algorithms for PV with energy storage systems (ESS), the main objective of the study is to evaluate the capacity to limit the RR and maintain SOC of BSS at the end of the day. The results have shown that an adequate control of the SOC can increase the BSS lifespan, it is important to mention that the authors have not considered SC in their study. PV variability mitigation by adaptive moving average control is presented in [12], adaptive battery SOC control maintains power output close to the reference signal. The experimental results have managed to reduce storage utilization during times of low variability. However, the authors mention that the proposed method produces significant delays in the forecast of PV energy. In grid-connected systems, the main objectives of the ESS are to balance the electric power flow between the source with the load and reduce power fluctuations, at the same time, the fast fluctuation requires a storage system with high power density, most authors conclude that the use of SC for this type of controls is important, in [13] a HESS composed of (BSS and SC) to meet the aforementioned requirements is proposed, the configuration can distribute the power demand between the different energy storages, the results show the feasibility of the proposed scheme. Nevertheless, computational times and experimental validations that demonstrate the effectiveness of the method are not considered.

The control strategy is an important factor that will influence the smoothing effect and the size of ESS, in Ref. [14] a novel control strategy to regulate the SOC of BSS is proposed. The results demonstrate that the strategy can smooth the PV power fluctuation effectively at low cost. On the other hand, the authors in [14] do not consider long-term PV fluctuations (e.g. one year) which could cause an oversizing of BSS. In addition, the use of BSS to reduce power fluctuations increases the complexity of the computational method because the SOC must be kept within certain established limits, Ref. [15] studies the impact of storage technologies, temporal resolution for a hybrid system PV-wind, the study concludes that the cost of energy is high considering various types of BSS. Battery cost variance, lifespan, BSS minimum SOC affect energy cost and computational effort. The advantages of using SC with respect to BSS to reduce power fluctuations is evident, the optimization methods when using SC are simpler since fewer control variables are required, one of the main characteristics of predictive control is the precision of the forecast data. In this regard, the Ref. [18] proposes a method to sizing optimization using publicly available Singapore power system data over long time intervals. The results show that the ESS can not only effectively control the rate of increase of PV power, also significantly reduce the spillage of PV power. In Ref. [16] the authors present a novel RR smoothing control methodology for low voltage power distribution networks with high levels of PV penetration, the novel method consists of controlling the RR applying the fast Fourier transform, the results show that the approach can manage the RR based on PV penetration. Nevertheless, the main limitation of this method is the longer time interval (hourly) used for power fluctuations where these appear in minutes or seconds. Similarly, in [17] the authors present a new power smoothing algorithm based on active and reactive power control for a PV and BSS, the reactive power control algorithm regulates the voltage on the grid side, again, the sampling time is restricted to one hour steps which could cause inaccuracy issues when evaluating faster power fluctuations. One of the main shortcomings of using BSS to reduce power fluctuations is the operating regime of the SOC, in [18] the authors have proposed a method of controlling the SOC of BSS through SC avoiding to operate at extreme levels of SOC an efficient response of BSS is achieved, likewise, the authors indicate that this procedure can cause a considerable increase in total costs and an oversizing of BSS. In Ref. [19] a power smoothing method using the SC is presented allowing to rich a higher level of penetration of wind turbines.

In the literature, power smoothing techniques are extensive, among the most studied are the moving average (MA) and RR methods due to their simplicity to implement and less computational effort [20]. However, these techniques can be improved with respect to several aspects, the Ref. [20] presents a novel strategy based on stepped rate control (improved RR) is proposed, which provides the most efficient use and with fewer cycles of ESS in situations that require several PV plants. The results show a better correction of the algorithm with respect to the common RR method since data sampling more accurately approximates the real power fluctuations. However, the study is limited to computational results. More recently, the authors in [21] present a SOC regulation strategy, the results show a close approximation to the real fluctuations of RES in exchange for a higher computational effort. In Ref. [22], a novel ramp rate limiting (RRL) control method to address existing gaps in the technical literature is proposed, the authors discuss the main advantage of the proposed method compared to a filter-based and MA methods in a techno-economic way considering several parameters, e.g., payback time, sizing optimization and SC cost, the proposed method is encouraging. Nevertheless, important issues such as the operability of the SC or the classification of power fluctuations are not addressed. Likewise, the authors in Ref. [23] mention the versatility of the RR method presenting some improvements, the method proposed by the authors is based on the exponential smoothing method, the results are compared with the MA method, the authors indicate that the MA exhibits a memory effect that makes BSS operates all the time. Thus, the proposed RR control strategy overcomes this limitation by operating the BSS only during significant fluctuations, the authors indicate that the MA method can suffer several inaccuracies when considering previous fluctuations to perform power smoothing. The approaches proposed by the authors indicate that the RR method would be beneficial for decision makers in electrical distribution companies company, being able to evaluate the options and adopt any of the RR control strategies based on implementation costs [24], applying the RR method, it was found that an ESS power rating of 60% of the PV string power rating is adequate to smooth almost all detected PV power ramps, even with strict RR limits [25]. Therefore, the trend in power smoothing methods lies in improving the SC control SOC, as the random characteristics of the power fluctuations could cause an oversizing in SC generating energy losses. To sizing optimization and operability of the SOC efficiently, a method of prediction and correction of fluctuations simultaneously is required.

According to the studies mentioned above, unlike BSS, the high power density of SCs makes them ideal for smoothing fluctuations, the fast charge/discharge cycles in BSS cause decrease its lifespan, making the renewable system more expensive in the long term [6]. In this context, the literature review suggests using SCs to smooth PV power fluctuations [26]. Some maximum ramp rates imposed by electric companies is e.g., 10%/min of PV power as in the case of Puerto Rico [27] the RR limit will depend on government policies and the configuration of the RES [28]. To improve power smoothing using SC, an improvement on RR and MA-based algorithms is suggested for long-term applications [29]. Several identified challenges are based on the reduction of the energy losses by the unnecessary use of the SC and the optimization of the computational effort in big data for short time steps [30]. The effective use of SC for the reduction of power fluctuations requires a thorough analysis of the efficiency of power storage and delivery, using real data and laboratory experiments with commercial equipment, it should also be considered that the level of fluctuation in the PV plant decreases as the size of the plant increases [31], as well as the improvement of the quality of the energy and the minimization of the voltage drop avoiding penalties by the electricity distribution company [32].

Summarizing, some research gaps have been identified regarding the sizing optimization and operability of SC to reduce power fluctuations. The forecast and classification of the rising and falling PV power peaks allows to effectively identify the SC capacity to correct the fluctuation of power generated by PV. Therefore, this paper presents a novel predictor-corrector power smoothing method (P – C) for small PV systems using SC. The new method aims to optimize and improve the conventional algorithms through a combination of the MA and RR methods with heuristic criteria. To validate the new method, exhaustive experiments in the microgrid laboratory of the University of Cuenca have been done [29].

The main contributions of this paper are the following:

In the first stage of the novel proposed method, a fluctuation forecast technique based on the reduction of scenarios (cluster) is presented, which uses a simple k-means algorithm application model based on unsupervised learning of the fluctuations generated in each time interval (year). This strategy allows optimizing the computational effort of the process and reduces energy losses by characterizing the type of fluctuation (rising and falling) allowing us to forecast the number of charges/discharges cycles of the SC. In the second stage, the power smoothing algorithm consists of a very-short-term power prediction for PV power based on the moving average MA that obtains a referential value for the SC, the algorithm calculates the average value of PV power variation over a number of periods and then corrects against the predicted reference power based on RR method (avoids accumulating unnecessary energy in the SC).

The experimental validation of the proposed method is done in a microgrid with PV capacity of 15 kWp and a SC capacity of 400 Wh connected to the grid using an energy management system (EMS) through MATLAB software, real-time data processing is done via Modbus communication (significantly improving the computational calculation and reducing delays).

The remainder of the paper is organized as follows:

Section 2 explains the proposed methodology, section 3 analyzes the PV power fluctuations and their ramp rate. Then, in section 4 the new power smoothing method is presented. Section 5 shows the main characteristics of the energy storage system under analysis. The results are discussed in section 6. Finally, section 7 concludes the paper.

Nomenclature

PV	Photovoltaic
SC	Supercapacitor
EMS	Energy management system
BSS	Battery Storage System
MA	Moving average
$R-R$	Ramp rate
PCC	Common Connection Point
SOC	State of charge
V	Two-column vector time step and ramp rate
$P-C$	Predictor-Corrective method
P_{GRID}	Grid power
P_{SC}	Supercapacitor power
P_{MA}	Output power average moving method
P_{ref}	Reference power value
P_{P-C}	Output power predictor corrector
P_{PV}	Photovoltaic power
P_{R-R}	Output power ramp-rate method
E_{SC}	Supercapacitor energy storage
$E_{SC\ discharge}$	SC energy discharge
$E_{SC\ charge}$	SC energy charge
SOC_{SC}	SC State of charge
SOC_{IC}	SC Initial State of charge
t	Time
Δt	Time interval
t (t)	Index for time periods
X_t	Output power of the PV installation (without smoothing) at instant t,
η_C	Performance during the storage charge process
η_D	Performance during the storage discharge process
CC	Reference power correction intensity modulation coefficient
R_{max}	Maximum Ramp Value
P_{charge}	SC power during the charging process
Δt_{charge}	Difference between two states of charge of the SC
SOC_{min}	SC minimum state of charge
SOC_{max}	SC maximum state of charge
P	Nominal power of the renewable system
NMA	Number of periods used to calculate the moving average
NMS	Number of periods used to calculate the variation in the energy contained in the storage
vs_t	Power transferred from the photovoltaic panels to storage in period t (cut peaks)
sr_t	Power transferred from storage to the grid in period t (fill gaps)
soc_t	Energy contained in storage at the end of period t
$\widehat{p_t}$	Reference power prediction value using the moving average method
Δsoc_t	Value of the average variation of power in storage
M_{ij}	Minkowski metric

2. Methodology

This paper presents a new power smoothing method to reduce PV power fluctuations using SC. The proposed methodology is shown in Fig. 1 and was developed as follows:

The introductory approach presents the real PV power fluctuations during a conventional day, classifying the imposed RR, PV and SC storage capacity. Then, the new power smoothing method is presented, consisting of two stages, prediction and correction (P–C). During the first stage, the reference PV power prediction value is calculated using the MA method, based on real data with 1 – s resolution for one year, a cluster analysis is executed through k-means algorithm to classify the PV fluctuations and the SC charge/discharge cycles are estimated. In the second stage, the reference PV power is generated using the very short-term MA method, these values are applied in the new power smoothing

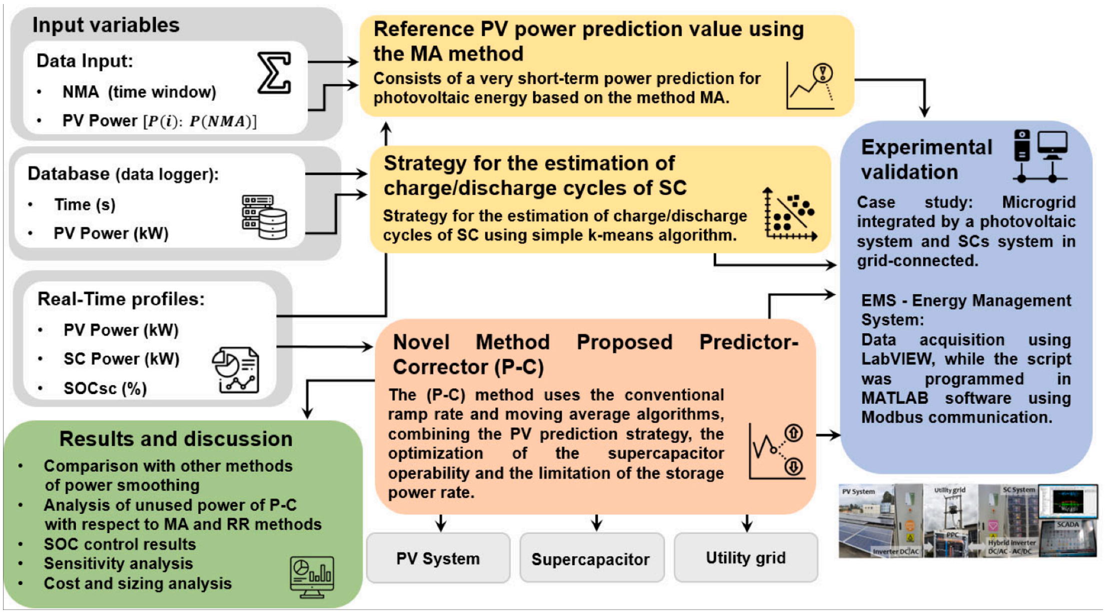

Fig. 1. Pictographic representation of the methodology proposed in this paper.

method using the conventional RR and MA algorithms, combining the PV prediction strategy, the optimization of the supercapacitor operability and the limitation of the storage power rate. The results are experimentally validated under various technical and economic criteria. Finally, several sensitivities analyze are presented.

3. PV power fluctuations and ramp rate

In this paper, the value of the PV fluctuations value is calculated using the RR method for the time step $t(i)$ shown in Eq. (1) and has been defined as the change in the PV output power between two successive time steps $t(i)$ and $t(i-1)$ [6,20,29,33].

$$RR(i) = \left|\frac{d}{dt}P_{PV}(i)\right| = \left|\frac{[P_{PV}(i) - P_{PV}(i-1)]}{t(i) - t(i-1)}\right| \tag{1}$$

A RR of ±10%/min of nominal PV power capacity to avoid a detrimental impact caused by fluctuations in the utility grid is imposed. Adequate use of SCs must be ensured by limiting and optimizing their energy capacity. Therefore, the number of charge/discharge cycles must be balanced with respect to rising and falling power peaks. Fig. 2 shows the PV power fluctuations in an ordinary day for a PV capacity of 15 kWp. The RR limit is set at ±10%/min of its nominal PV power (±1.5 kWp) and SC with a capacity of 400 Wh. Therefore, it can be observed that at certain hours of day, positive ($RR(i) > 1.5\ kW/min$) and negative ($RR(i) < -1.5\ kW/min$) fluctuations are generated. For this reason, it is necessary to analyze the PV fluctuations in detail.

4. Novel method proposed predictor-corrector (P-C)

The new algorithm has two stages, prediction and correction, in the first stage the reference power is obtained by predicting values $\widehat{p}t$, i.e., applying MA power smoothing method for a certain number of periods for steps $t(i-1)$. For the second stage, the SC must store enough energy to maintain the power smoothing band at suitable levels to overcome rising and falling PV fluctuations, the sampling rate for this study is 1 s.

4.1. Stage 1: Prediction

4.1.1. Reference PV power prediction value using the MA method

At this stage, the proposed method performs a short-term PV power prediction using the MA method, the result is the previous average values of PV power X_t input, during a certain interval NMA (number of periods used to calculate the moving average), designated by the user. The optimal value of the time window is adjustable depending on the RR

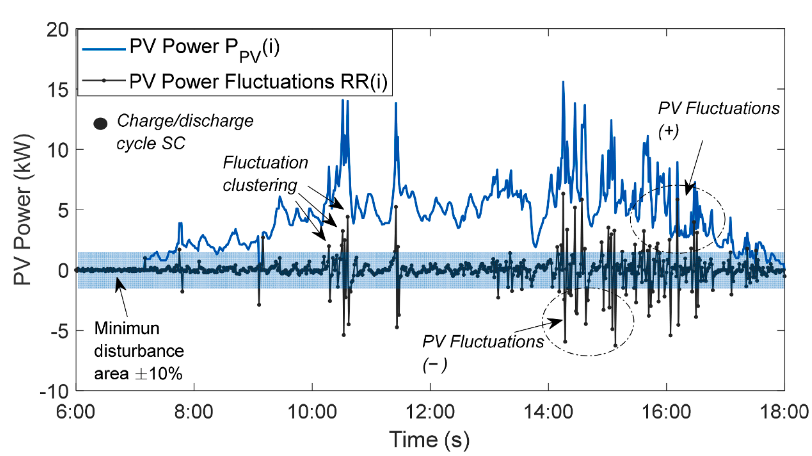

Fig. 2. PV output power and power fluctuations disturbance, daily sampling interval with seconds time steps.

limit. In this prediction stage, a value of NMA = 10 min is initially assigned. The reference power prediction value using the moving average method can be calculated with Eq. (2):

$$\widehat{p}_t = \frac{1}{NMA}\sum_{\tau=1}^{NMA} X_{t-NMA+\tau-1} \quad (2)$$

4.1.2. Strategy for the estimation of charge/discharge cycles of SC

To determine the number of SC charge/discharge cycles during a certain time interval, the PV power fluctuations must be estimated. In this context, the exploratory technique based on cluster analysis to calculate the number of positive (+) and negative (−) PV fluctuations generated during a year through Eq. (1) has been used [34]. The PV fluctuations are classified with the application model of the simple k-means algorithm. In this way, positive fluctuation events can be interpreted as excess generation and it is considered useful energy to establish a charge cycle of the SC. Otherwise, negative fluctuation events can be considered as a power requirement and a discharge cycle of the SC is setting. The database corresponding to September 2019 is stored as a vector =[$t(i)$; $RR(i)$], (i.e., the number power fluctuations exceed the RR limits during an interval) through the Waikato Environment for Knowledge Analysis (WEKA) software platform and MATLAB [34]. In this first stage, the cluster is evaluated for a month, cluster data using the k-means algorithm can use the Euclidean distance with Minkowski metric from Eq. (3). Thus, centroids are computed as the component-wise median rather than mean [21].

$$M_{ij} = \left\{\sum_{k=1}^{N} |a_{ki} - a_{kj}|^p\right\}^{1/p} \quad (3)$$

where: a_{ki} is the kth component of the n-dimensional vector a_i, which is the centroid of cluster i and j, only values $p = 2$ (Euclidean metric) [34].

Table 1 indicates the number of clusters and event based on the fluctuation percentage of the PV system. In the database of the vector $V = [t(i); RR(i)]$, a classification of 11 clusters is established (0, 1, 2, 3, 4, 5, 6, 7, 8, 9, 10) corresponding to September, where it is observed that cluster 9 contains approximately 51% of the data, these values correspond to night hours where the PV power output is zero, situating its centroid at a value close to zero of −0.002. On the other hand, cluster 1 and 2 are classified at the limit of PV fluctuations (±10%/min) with a percentage of 18% and 19% of the database, this indicates that their centroids are located at −0.15 and 0.13 for negative and positive PV fluctuations, respectively. Therefore, when adding the total values clusters 1, 2 and 9 generate a total of 37,086 data that would not be considered for mitigation, since these values are within the limit of ±10%/min in the fluctuation range and is discarded as SC charge/discharge cycle reducing computational effort.

In order to estimate the number of SC charge and discharge cycles, the rest of the clusters must be considered. That is, to reduce the PV fluctuations with RR from 10.1%/min to 25%/min (clusters 5 and 8), 814 charge cycles and 1130 discharge cycles are required for the SC, respectively.

Fig. 3 shows the result of the cluster analysis for PV fluctuations (Sep 2019) when the simple k-means algorithm is applied. According to Table 1, the number of cycles required for SC operation can be obtained according to its range of PV fluctuations reduction by adding the events of the range greater than 10%/min, (clusters 0, 3, 4, 5, 6, 7, 8 and 10), the results shows that the total charge/discharge cycles of the SC is 4675/month. In this way, it has been possible to estimate the number of SC cycles to reduce PV power fluctuation and the impact on the grid. The procedure is the same for the rest of the year. Fig. 4 shows the summary of the study that allowed us to estimate the number of charge/discharge cycles required to limit the different percentages of RR value. The curve remains similar throughout the year with respect to the number of occurrences, and decreases depending on the percentage of fluctuation reduction. At the 10%/min benchmark, the maximum number of cycles is 11,181/month with the highest percentage of fluctuations. April is the month with the lowest number of cycles, with 5000/month. This indicates a necessary operation of approximately 167/day charge/discharge cycles in this month. On the other hand, for a 20% reduction, its number of cycles would be approximately half as indicated in Fig. 4. In this way, positive and negative RR limit parameters are set to control the SC's SOC. Therefore, it is possible to classify the PV power fluctuations according to the maximum required RR, operating the SC only when the fluctuation exceeds the RR, reducing the unnecessary charge/discharge of the SC. In the next stage, SC state of charge levels are maintained within a "smoothing band" further controlling SC operability.

4.2. Stage 2: Correction

In this stage, the reference power is generated based on the conventional RR method, the stored energy Δsoc_t is calculated, followed by the average value of the energy variation over a certain number of periods for steps $t(i-1)$. This value is corrected with respect to the predicted reference power, obtaining a new term (p_t).

4.3. Control scheme

Fig. 5 shows the control scheme of the new proposed method including the two stages (prediction and correction), as can be seen, the possible situations are:

- If in the steps $t(i-1)$ (periods considered for the calculation of Δsoc_t) the SC has been charged, the correction of the reference power consists in increasing this value to use it in the following time interval and maintain a steady energy level.
- If in the steps $t(i-1)$ (periods considered for the calculation of Δsoc_t) the SC has discharged, the correction of the reference power consists in reducing this value to accumulate energy in the following interval.

Table 1
Cluster analysis for PV fluctuations (september-2019) simple k-means algorithm.

Item	PV Fluctuation Range	N° Cluster	Data	Time	Centroids	Data number or events	Estimate for SC cycle
1	0% (±)	9	51%	22:06	−0.002	21,455	N/A
2	0.1% to 10% (−)	1	18%	01:00	−0.15	7551	N/A
3	0.1% to 10% (+)	2	19%	14:30	0.13	8080	N/A
4	10.1% to 25% (−)	5	2%	20:48	−0.97	814	Charge
5	10.1% to 25% (+)	8	3%	05:32	0.84	1130	Discharge
6	25.1% to 50% (−)	4	1%	16:58	−2.59	455	Charge
7	25.1% to 50% (+)	0	1%	12:32	2.47	453	Discharge
8	50.1% to 80% (−)	6	1%	14:52	−5.60	445	Charge
9	50.1% to 80% (+)	10	1%	12:01	5.50	443	Discharge
10	80.1% to 100% (−)	3	1%	13:18	−10.83	462	Charge
11	80.1% to 100% (+)	7	1%	08:58	10.77	473	Discharge

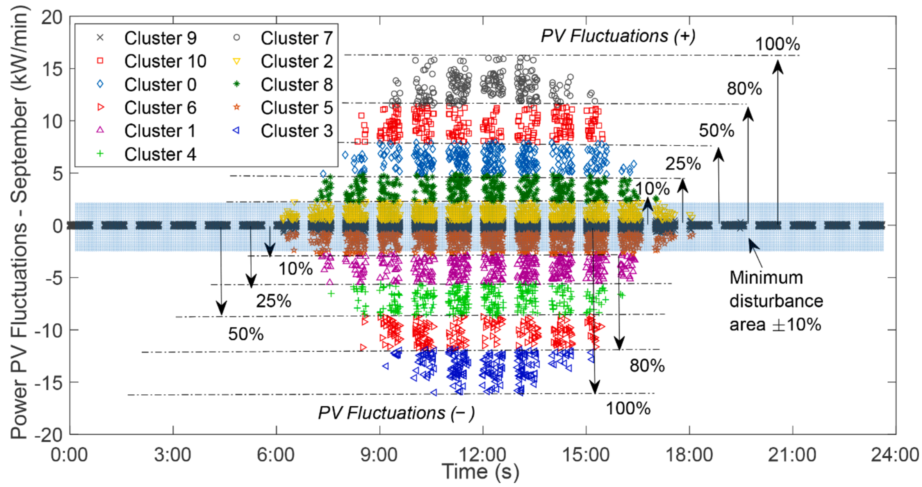

Fig. 3. Cluster analysis of PV power fluctuations in September 2019.

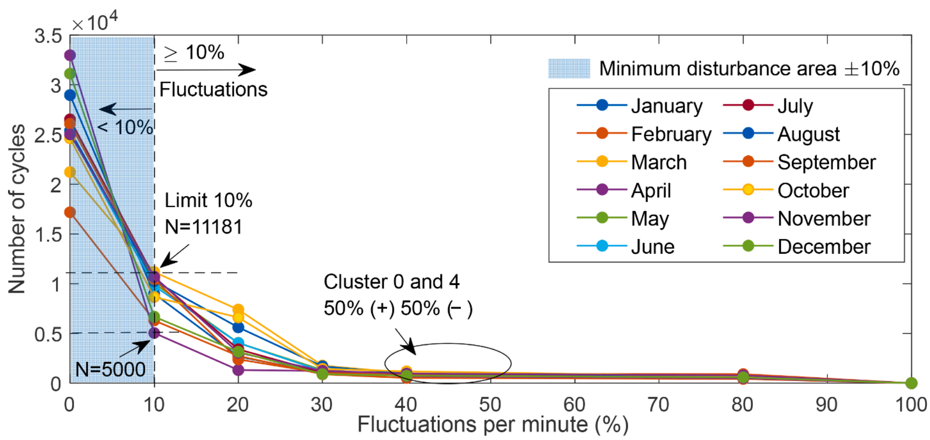

Fig. 4. Forecasted SC charge/discharge cycles for one year.

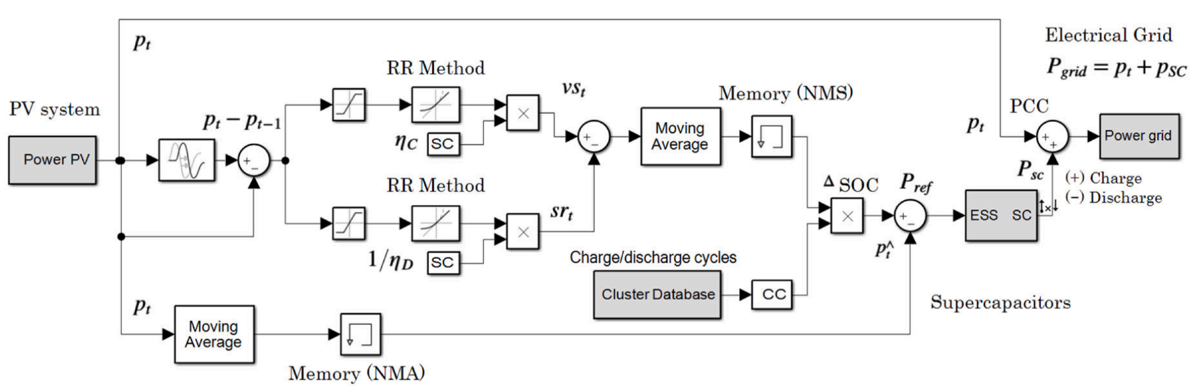

Fig. 5. Control scheme of the new proposed power smoothing method (P-C).

To calculate the allowable power variation in each interval, a "strict" interpretation of the RR limit is made for each step (Δt), and the maximum allowable PV power variation is $\pm P \times R_{max} \times 60 \times \Delta t$. This is not the only possible interpretation; the RR limit could also be applied for longer intervals. However, if the PV power variation is less than the admissible limit of RR (10%/min), the algorithm is not enabled.

In order to determine the values vs_t and sr_t, for the first time step, i.e., ($t = 1$), the reference power given by the MA $(\widehat{p_1})$ is used. Thus, for time steps $t > 1$, the new reference value (p_1) allows us to predict the power exchanges between PV, SC and the grid. The explanatory algorithm of the proposed method is shown in Fig. 6. If the reference power does not meet any of the conditions shown in Fig. 6, p_t is adjusted to the corresponding limit, i.e., $p_t + P \times R_{max} \times 60 \times \Delta t$ or $p_t - P \times R_{max} \times 60 \times \Delta t$.

The NMS index expresses the number of periods to calculate the variation of the energy stored in SC, in this case NMS = 5 min is assigned, this value determines the average variation of SC state of charge (Δsoc_t). Then, considering the predicted PV fluctuations and the SC charge/discharge cycles, the SC reference signal is set.

The algorithm shown in Fig. 6 is explained below:

1. Data Input

1.1: Constant data: $P, R_{max}, \Delta t, , NMA, NMS, \eta_C, \eta_D, CC, , SOC_{MIN}, SOC_{MAX}$

1.2: Variable data: p_t, X_t, SOC_{SC}

2. Restriction of use of PV inverters:

2.1: If $p_t \leq 0$

2.2: $P_{ref} = 0$

2.3: End if

3. Restriction of ramp-rate (+) and (-)

3.1: If $|p_t - p_{t-1}| > P \cdot R_{max} \cdot 60 \cdot \Delta t$

3.2: If $p_t - p_{t-1} > 0$

3.3: $X_t = p_{t-1} + P \cdot R_{max} \cdot 60 \cdot \Delta t$

3.4: Else $X_t = p_{t-1} - P \cdot R_{max} \cdot 60 \cdot \Delta t$

3.5: End if

3.6: End if

4. P-C method and control system for SC

Data processing:

Reference PV power prediction value using the MA method

4.1: $\widehat{p_t} = \frac{1}{NMA}\sum_{\tau=1}^{NMA} X_{t-NMA+\tau-1}$

*NMA initial memory time required (10 min)

Power transferred from the photovoltaic panels to storage in period t (cut peaks)

4.2: $vs_t = max\{0, X_t - (p_t + P \cdot R_{max} \cdot 60 \cdot \Delta t)\}$

Power transferred from storage to the grid in period t (fill gaps)

4.3: $sr_t = max\{0, (p_t + P \cdot R_{max} \cdot 60 \cdot \Delta t) - X_t\}$

Value of the average variation of power in storage

4.4: $\Delta soc_t = \frac{1}{NMS}\sum_{\tau=1}^{NMS}\left(\eta_C \cdot vs_{t-NMS+\tau-1} - \frac{1}{\eta_D} \cdot sr_{t-NMS+\tau-1}\right)$

*NMS initial memory time required (5 min)

*Charge and discharge efficiency parameters η_C and η_D

Reference power to SCs

4.5: $p_{ref} = \widehat{p_t} + CC \cdot \Delta soc_t$

*CC correction intensity modulation coefficient [0-5]

5. Restriction of SOC for SC and reference power assignment

5.1: If $SOC_{MIN} \leq SOC_{SC} \leq SOC_{MAX}$

5.2: $P_{SC} = p_{ref}$

5.3: Else $P_{SC} = 0$

5.4: End if

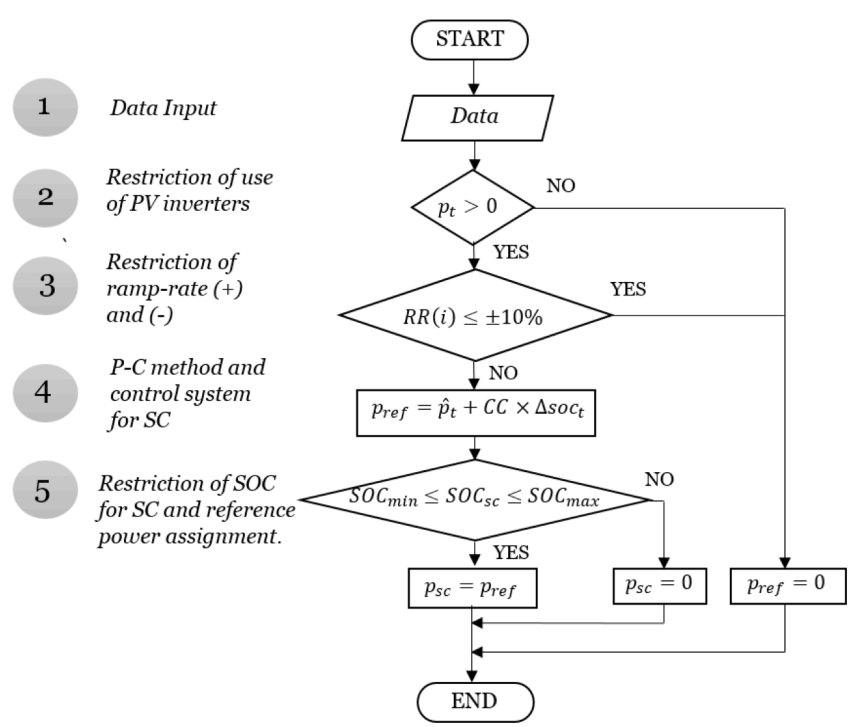

Fig. 6. Overall flowchart of the proposed controller.

It should be noted that in steps 4.1 and 4.4 an initial memory time of 10 min and 5 min respectively is required, due to the temporary registration of the MA method. After that period, the algorithm generates the values in real time based on the average of the previous values. This process does not affect the execution of the algorithm in the mitigation of fluctuations during this period, since the code can be executed a few minutes before the photovoltaic generation, for example 05:50 h. After obtaining the vector of values and its average, the p_{ref} is calculated in real time with a minimum computational requirement.

5. Energy storage system characteristics

In this paper, Electrical Double Layer Capacitor (EDLC) type SCs are considered for their high power density and commerciality. In addition, this type of SC is available in the laboratory of the University of Cuenca where the experimental validations of the new proposed method have been done.

The specific power available of SC (P_d) according to IEC 62391–2 is defined by the Eq. (4):

$$P_d = \frac{0.12 \times V^2}{ESR_{DC} \times mass} \tag{4}$$

where: V is the SC voltage, ESR_{DC} is the equivalent series resistance, *mass* is the typical mass.

The energy stored (E_{SC}) in the SC is defined by the Eq. (5):

$$E_{SC} = \frac{\frac{1}{2} C \times V^2}{3600} \tag{5}$$

where: C is the capacitance of SC.

It is evident that the current-voltage relationship of the SC differs from the conventional capacitor ($I = Cdv/dt$, $E = CV^2/2$) due to fractional dynamics. A generalized approach to evaluate SC efficiency under fractional order variation resulting from different operating conditions (charge/discharge cycles, current magnitude and time) has not been presented in the literature. Analysis for different operating conditions requires the extraction of fractional order model parameters from the experimental data based on which power and energy during the charge and discharge phase can be evaluated [24]. In this paper, the efficiency of the SC has been evaluated, in terms of energy stored and transferred during charge and discharge, respectively.

Table 2
Technical parameters of the equipment used in the experiment.

System type	Model	Cells / Modules	Operating voltage	Capacity	Capital Cost
PV	Atersa 250 Polycrystalline	60 (15 × 4)	150 Vdc-450 Vdc/ 230 Vac	15 kW	1000 (USD/ kW) [36]
SC	Maxwell BMOD-0130 130F	10 Modules	420 Vdc-560 Vdc/ 230 Vac	0.4 kWh	27.5 (USD/ Wh) [37]
Utility grid	Three-phase 60 Hz	N/A	230 Vac	N/A	N/A

6. Results and discussion

6.1. Case study

The experimental validation of the new proposed method has been done in the microgrid laboratory of the University of Cuenca shown in Fig. 7 [35]. The overall characteristics of the equipment are presented in Table 2. Energy Management System (EMS) performed the data acquisition using LabVIEW, while the script was programmed in MATLAB software using Modbus communication. The data acquisition time was milliseconds, which produced a fast response in the system, avoiding delays.

To illustrate the basic principles of the proposed energy management controller, charge/discharge experimental tests of the SC were performed under various power values (± 30 kW, ± 20 kW, ± 10 kW and ±5 kW) as shown in Fig. 8. The results show the behavior of the voltage and current during the SC charge and discharge cycles, the power smoothing band indicates the lower and upper limits in which the SC will perform power smoothing. The minimum SOC of SC is set to 5%, because the SC needs an initial charge to start its operation, the maximum SOC of SC is 95% since the SC needs to store at least 5% of charge to start operating the next cycle. Therefore, the power smoothing band is defined between 5% – 95%. In this way, the charge and

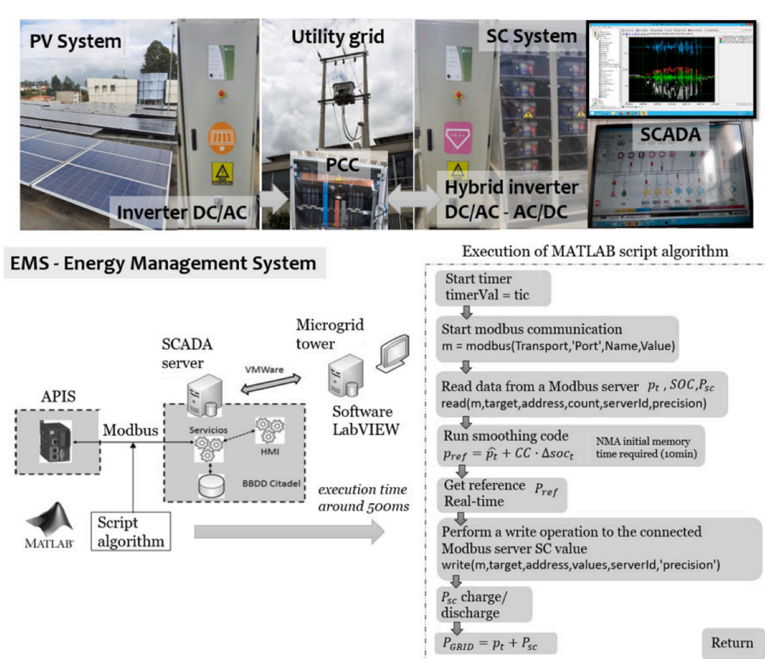

Fig. 7. Schematic representation of the test bench in microgrid laboratory of the University of Cuenca.

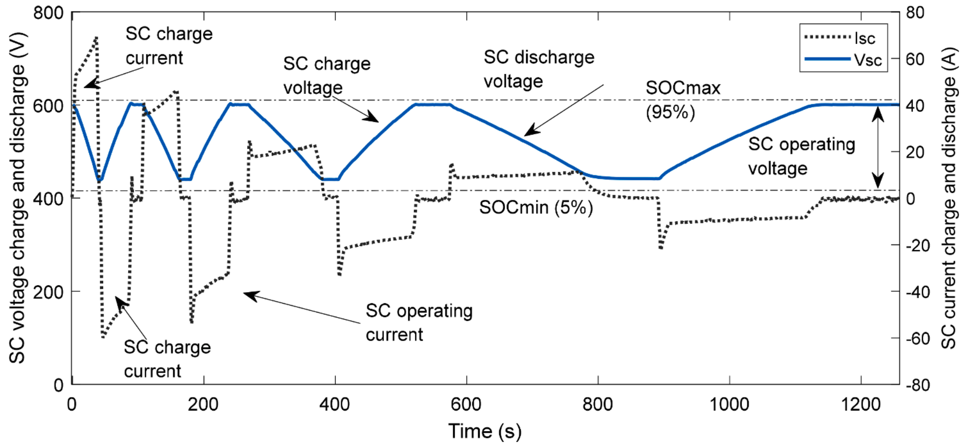

Fig. 8. Testing of charge/discharge cycles of the SC in the laboratory.

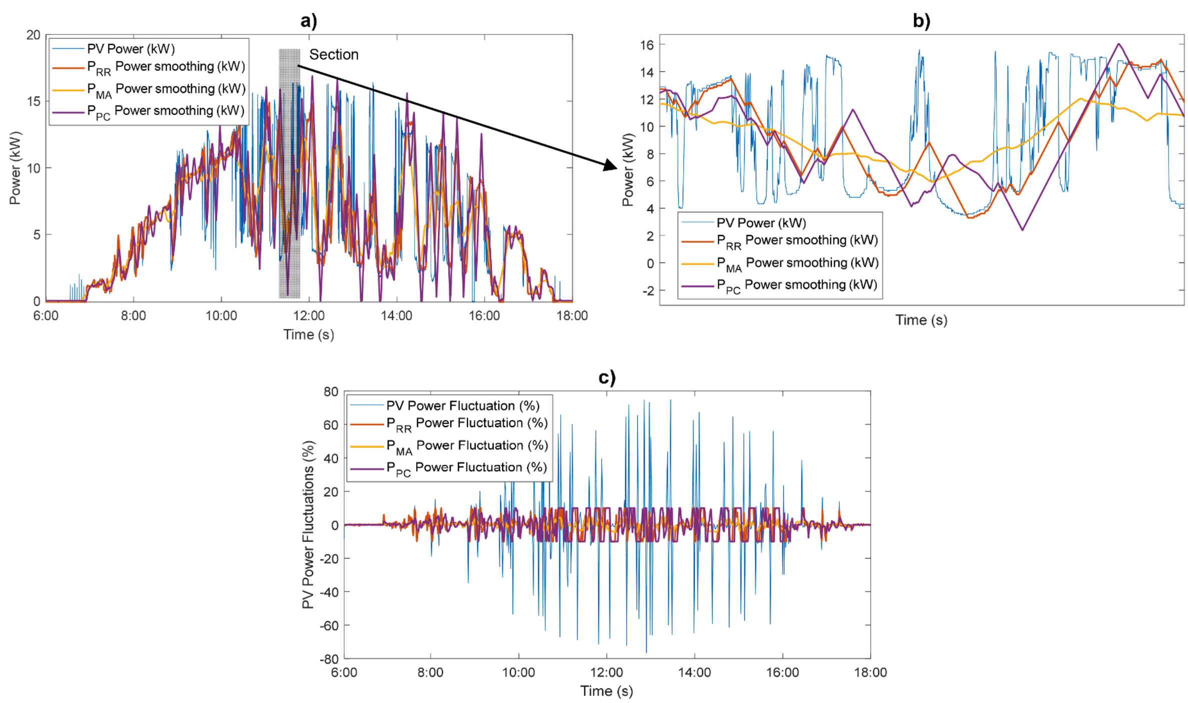

Fig. 9. Comparison of the power fluctuations of the novel power smoothing method (P-C) with respect to the R-R and MA methods: (a) PV power fluctuation in (kW), (b) zoom section of PV power fluctuation in (kW), and (c) PV power fluctuations in (%).

discharge efficiency parameters η_C and η_D can be estimated with values around 94% and 93%, respectively. It is important to note that, in this case, the SC operates in a range of 440 V– 600 V and the voltage drops to zero, the SC requires an external initial charge to operate again because of the characteristics of the grid-connected inverter.

6.2. Comparison with other methods of power smoothing

To validate the new proposed method, this section presents a comparison with two conventional algorithms: MA and RR. The first of them is explained in detail in Ref. [8] and [23]. Similarly, Ref. [38] analyzes the RR method. Fig. 9 shows the experimental results using the three methods. It is important to mention that the experimental analysis of fluctuations has been done with a sampling resolution of 1 s. The comparison clearly shows the ability of the method to overcome PV power fluctuations, the term "unused power" expressing the unused PV power after applying a power leveling method (power losses). Moreover, in Fig. 9 (c), the fluctuations of PV (%) are presented for the MA, RR and P-C methods, with the limit of RR ±10%/min. Then, the algorithm is executed with a dimensioned value defined to validate allowed RR violations when the SOC of the SC is exceeded. That is, having a value of $P_{ref} \neq 0$ and the value of the SC must be $P_{SC} = 0$ when it exceeds the SOC_{max} or SOC_{min} defined.

In certain cases, it is not necessary to use SCs due to the algorithm's resolution and ability to detect power fluctuations. In such cases, according to the proposed P – C method, when considering the SOC as a controllable variable it is possible to maintain the power smoothing band within the pre-established limits due to the predictor-corrector characteristic of the method, which would optimize its use, according to the RR defined.

Therefore, the operability of the SC is reduced with respect to the MA and RR methods as shown in Fig. 10. The SOC control causes the SC to operate when the RR of the fluctuations is greater than ±10%/min, avoiding unnecessary charge/discharge cycles as in the MA and RR methods.

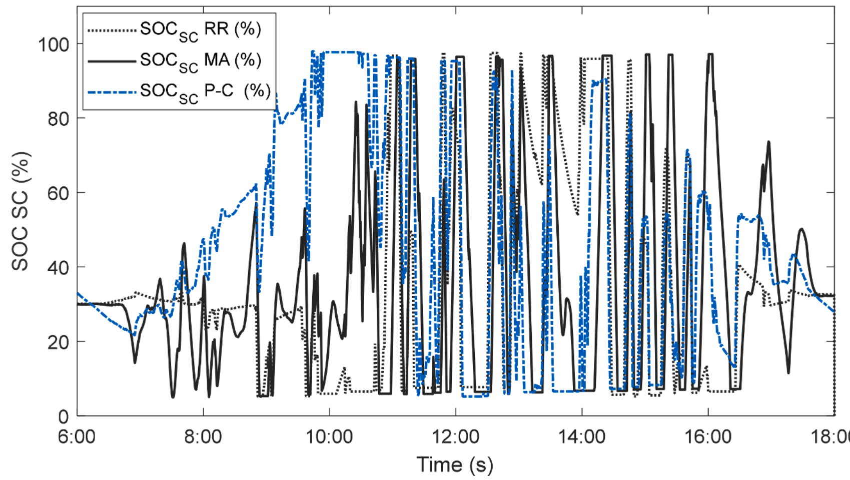

Fig. 10. State of charge of novel method (P – C) with respect to the MA and RR methods.

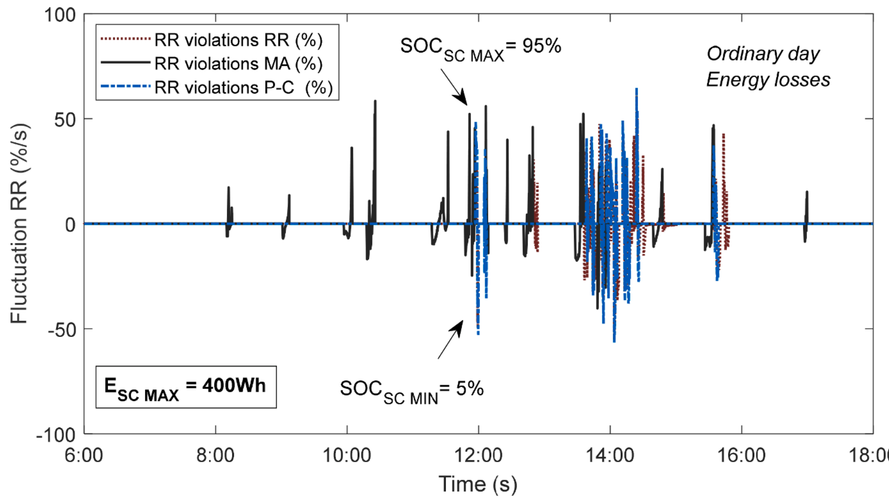

Fig. 11. Loss power and ramp rate violation for the proposed method (P – C) with respect to the MA and RR methods, PV = 15 kWp and SC = 400 Wh.

Table 3
Energy losses and technical violations under different sky conditions.

Day	MA kWh/day	Number Technical Violations MA	RR kWh/day	Number Technical Violations RR	P – C kWh/day	Number Technical Violations P-C
Ordinary day	2.06	92	2.13	47	2.03	34
High cloudiness	0.67	61	0.05	6	0.04	2
Little cloudiness	9.09	193	8.03	202	5.26	171
Clear day	0.035	12	0.003	0	0.0017	0
Semi-clear day	1.3	130	1.19	158	0.26	33
Total	13.155	488	11.403	413	7.5917	240

6.3. Analysis of unused power of P-C with respect to MA and RR methods

In the case study, the capacity of the SC of the laboratory has been determined at 400 Wh, the PV power peaks will exceed the RR of ±10%/min in certain cases. The result can be seen in Fig. 11, where fluctuations with RR greater than ±10%/min (RR violations), PV = 15 kWp and SC = 400 Wh are represented. The comparison with the three cases under study is presented and the importance of managing an adequate SOC to mitigate fluctuations is emphasized [27].

As explained above, the predictive-corrective characteristic of the new proposed method avoids the unnecessary use of SCs in certain conditions by setting the SCs output power value as a reference P_{SC}. Thereby, Table 3 shows the quantitative values of energy losses (Wh/day) for each comparative methods and the PV energy generated during the classification of sky conditions; ordinary, high cloudiness, low cloudiness, clear and semi-clear considering a maximum value of ESS for the SCs of 400 Wh. The results show that the new method can reduce energy losses with respect to MA and RR. Table 3 shows the number of technical violations of the new power smoothing method proposed with respect to the MA and RR methods. For the comparison to have the same reference point, the SC capacity has been kept constant (400 Wh), it is evident that the new P – C method generates fewer technical violations with respect to the conventional methods (MA and RR).

6.4. SOC control results

Fig. 12 shows the response of the SOC control algorithm. The initial SOC of the SC is SOC_{IC} = 10% according to the reference power P_{ref} =

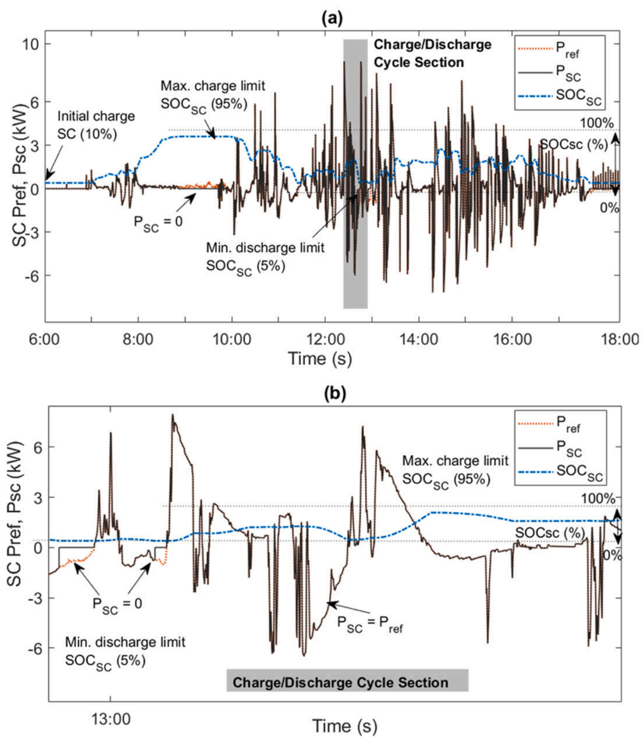

Fig. 12. Boundary conditions of SOC control: (a) control scheme for charge and discharge limits for SC, (b) zoom for the operating section of the SC cycle.

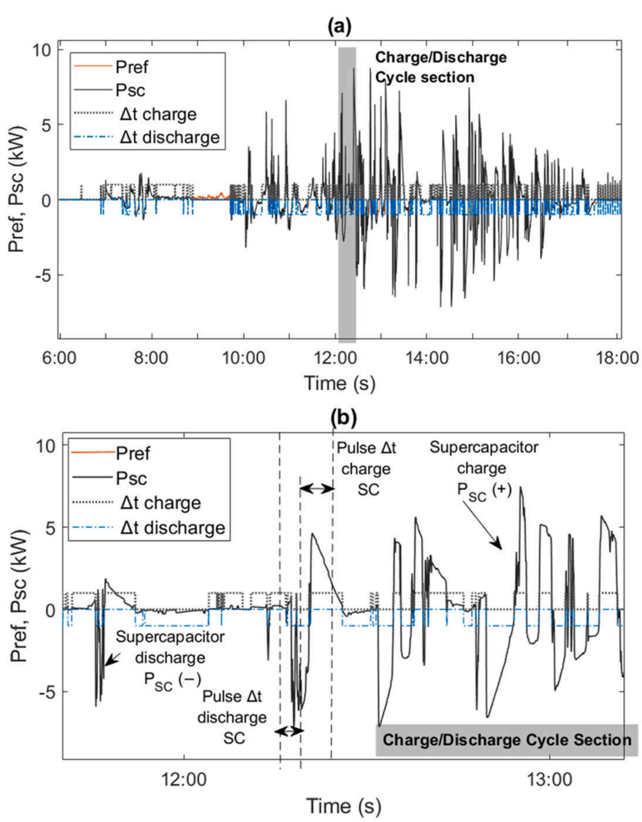

Fig. 13. Setting of time intervals for the control of the state of charge: (a) charge and discharge limits for SC, (b) zoom for the operation charge/discharge cycle section.

Table 4
Variable NMA values results in 5, 10, 15, 20 and 30 for a constant value of NMS = 5 (lower in energy Wh).

NMA	Ordinary day	High cloudiness	Little cloudiness	Clear day	Semi-clear day
5	439.89	202.32	1840.9	61.45	647.39
10	454.96	211.91	1817.8	60.85	634.37
15	499.16	215.07	1822.2	61.01	619.68
20	525.69	221.21	1778.1	61.13	598.52
30	508.65	226.29	1726.4	60.46	599.47

$P_{PV} - \{P_{MA}, P_{R-R}, P_{P-C}\}$. The difference with the PV power input indicates the energy required for the reduction of fluctuations predefined by the power smoothing method. However, the energy stored by the SC is limited by its upper SOC limit ($SOC_{max} = 95\%$), i.e., $P_{SC} = 0$ at 8:50 h – 9:30 h. In the same way, when $SOC_{min} = 5\%$, $P_{SC} = 0$ at 12:50 h – 13:10 h. To overcome this issue, the P_{ref} is replaced by the P_{SC} according to the allowed values of the minimum and maximum limits of the SOC.

The SOC control algorithm for limiting the power smoothing band initially assigns the value of P_{ref}, as the difference between PV output power and PV smoothed power. If the reference value is ($P_{ref} \geq 0$) the SC starts the charging process in an interval of $\Delta t_{charge} = t_2 - t_1$ in the positive cycle and defines $P_{sc} = P_{ref}$. In the same way, if the reference value is ($P_{ref} < 0$), the SC starts discharging process. This SC control algorithm for charge and discharge limits for SC is presented in Fig. 13.

6.5. Sensitivity analysis

6.5.1. Sensitivity analysis for NMA and NMS indices

Sensitivity analysis studies the impact of a dependent variable with respect to the evolution of certain indices. In this case, the application of the proposed power smoothing method (P−C) is analyzed under different values of (NMA) and (NMS) for day classification. The results show that for days of ordinary cloudiness and high cloudiness, the NMA = NMS = 5 match the minimum energy value. On the other hand, days of low cloudiness and clear days match NMA = 30 and NMS = 5. For semi-clear days, the minimum energy value parameters are NMA = 30 and NMS =30. Table 4 and Fig. 14 shows the results. In summary, the values to setting the minimum energy value can be defined with NMA = 10 and NMS = 5, which can be applied to the five cases described.

The results of the sensitivity analysis with respect to the reference power correction intensity modulation coefficient (CC), NMA, and capacity storage are shown in Fig. 15 and Fig. 16 for: (a) high cloudiness days; (b) low cloudiness days and (c) semi-clear days respectively. The SC energy change (Wh) obtains its minimum value in the range of [0–5] for the variable CC, which indicates that it is suitable to define a short period. In addition, to determine the optimal storage size of (SC) Eq. (6) is used.

$$b = max_t(SOC_t) - min_t(SOC_t) \quad (6)$$

Considering the days of high fluctuations during a year, the optimal SC capacity is around 2 kWh, for a PV system (15 kWp) connected to the grid as shown in Fig. 16 (c). In this way, it is possible to mitigate power fluctuations with a RR of 10%/min of the PV capacity. However, when considering the events for the little cloudiness day (Fig. 16 (c)), the periodicity is low. Therefore, the SC optimal sizing for an ordinary day (Fig. 16 (a)) is 450 Wh.

6.5.2. Sensitivity analysis with established SC sizing

In this section, the day with the greatest fluctuations (little cloudiness) is considered. In which different numbers of periods are established for the calculation of the MA in the PV (NMA) prediction and the number of periods for the variation of the energy contained in the NMS storage. These results are presented in the Fig. 17, the minimum values of $NMA = 10$ and $NMS = 5$ are indicated, for different values it can

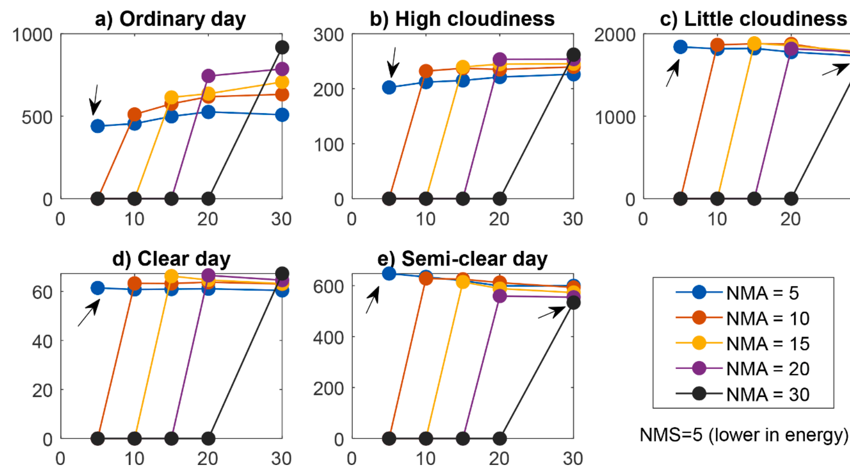

Fig. 14. Sensitivity analysis with respect to variable NMA at 5, 10, 15, 20 and 30 for a constant value of NMS = 5 (lower in energy), horizontal axis NMA and vertical axis energy (Wh).

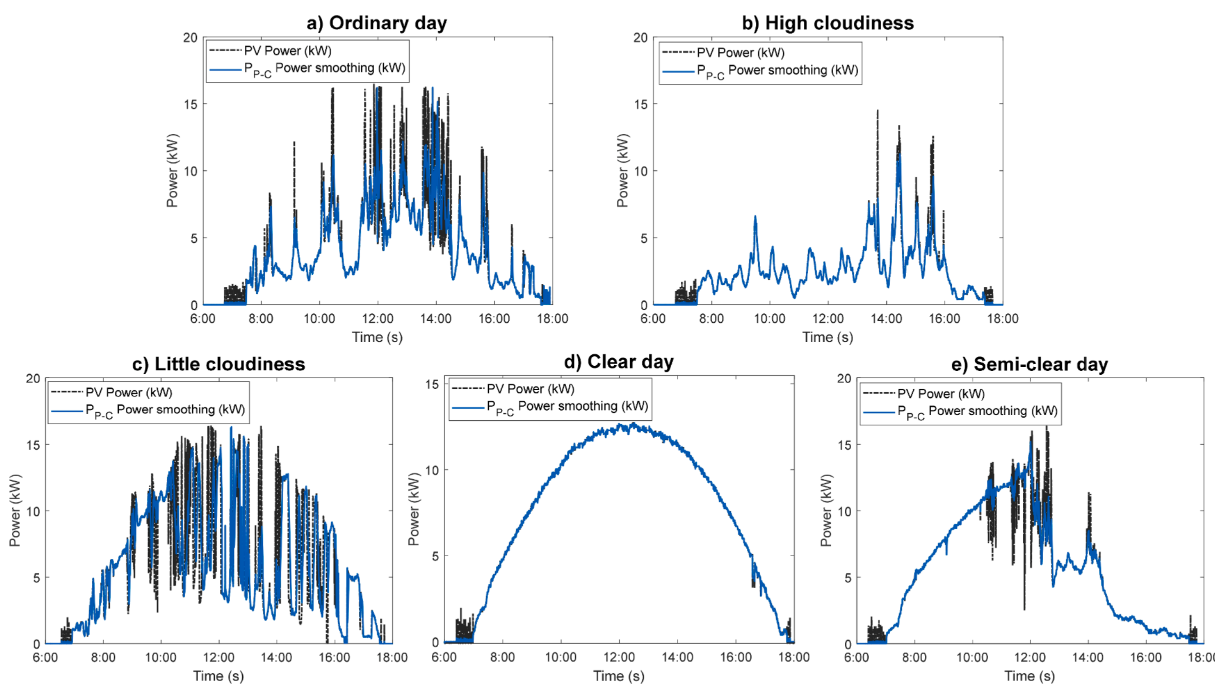

Fig. 15. Sensitivity analysis of the novel P-C method for different sky conditions.

produce an increase in energy losses (PV = 15 kWp and SC = 400 Wh).

6.5.3. *Sensitivity analysis for ramp rate values less than 10%*

In the novel proposed algorithm, it is possible to change the value of RR limit (RRL). However, it should be considered that for RR < ±10%/min, an increase in the SC capacity and the number of charge and discharge cycles, (see Fig. 4). Nevertheless, the RR limit is adjusted by the modulation coefficient of the correction intensity. In Fig. 18 a sensitivity analysis with respect to the energy storage capacity and the reduction of power fluctuations for different scenarios is presented, the PV system of 15 kWp capacity is analyzed. In this case, the day with the greatest power fluctuations (little cloudiness) is studied, the curve potentially grows as an approximation of $E(x) = E_m \times x^{-\alpha}$, where Em determines the maximum level of reduction α exponential parameter and x the desired fluctuation percentage.

6.6. *Economic analysis*

This section presents an economic analysis of the new proposed method, according to the costs shown in Table 2, the PV system has a total cost of USD 15,000 and the SC has an approximate cost of 27.5 USD/Wh. The total capacity of SC depends on several factors such as the ramp rate, the frequency of events where the PV power peaks exceed the RR limit or the weather conditions. In this case, the accumulated annual frequency of occurrence is considered as an index to calculate the optimal size of SC, for this, PV generation ranges are established to characterize the days of greatest annual occurrence according to the PV energy generated. The results show that for one year the PV fluctuations reach RR of ±78.20%/min with occurrence frequency as shown in Table 5.

In order to characterize the days of cumulative annual occurrence frequency. PV production is classified according to different ranges and under different climatic conditions as follows: high cloudiness = (0–30) kWh, ordinary day = (30–50) kWh, semi-clear day = (50–80) kWh and

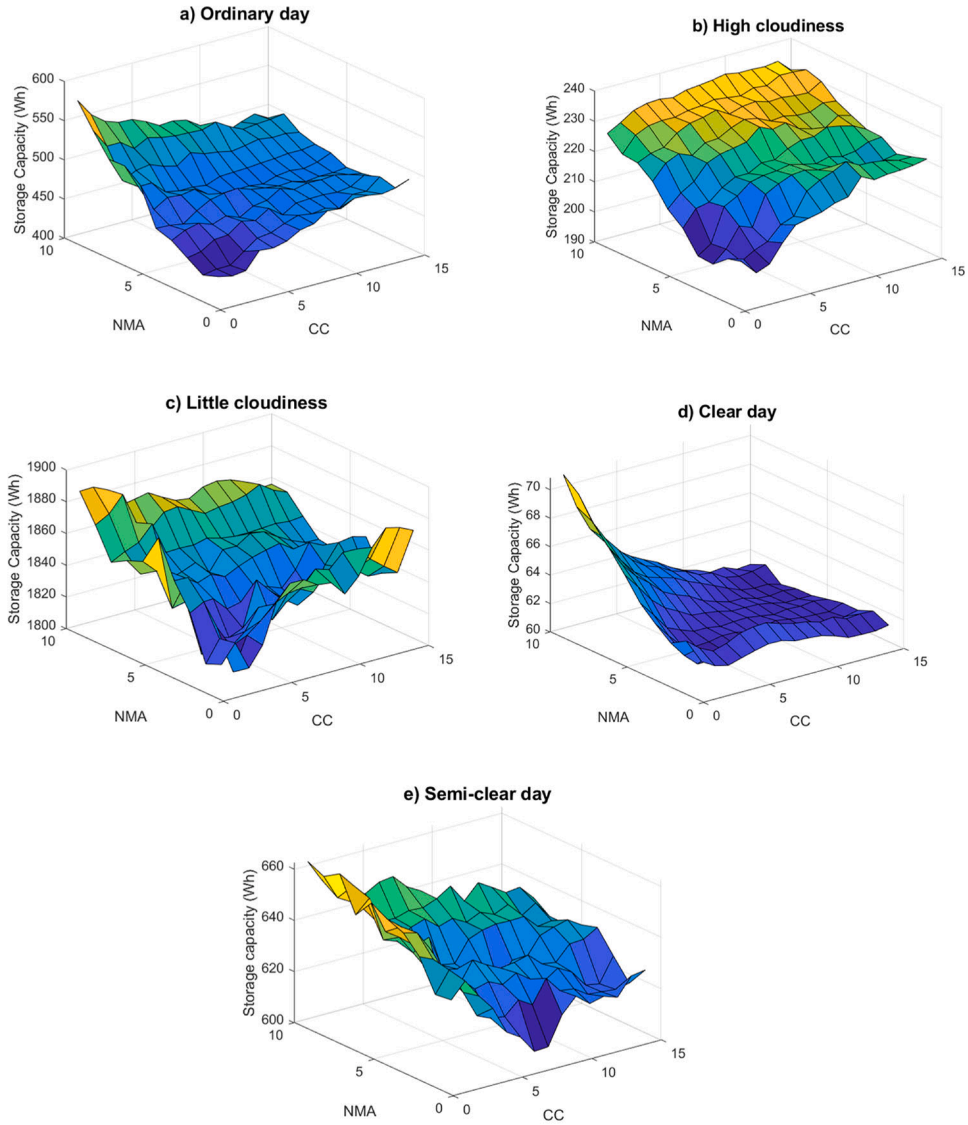

Fig. 16. Sensitivity analysis of novel P-C method for different scenarios: NMA vs CC vs storage capacity.

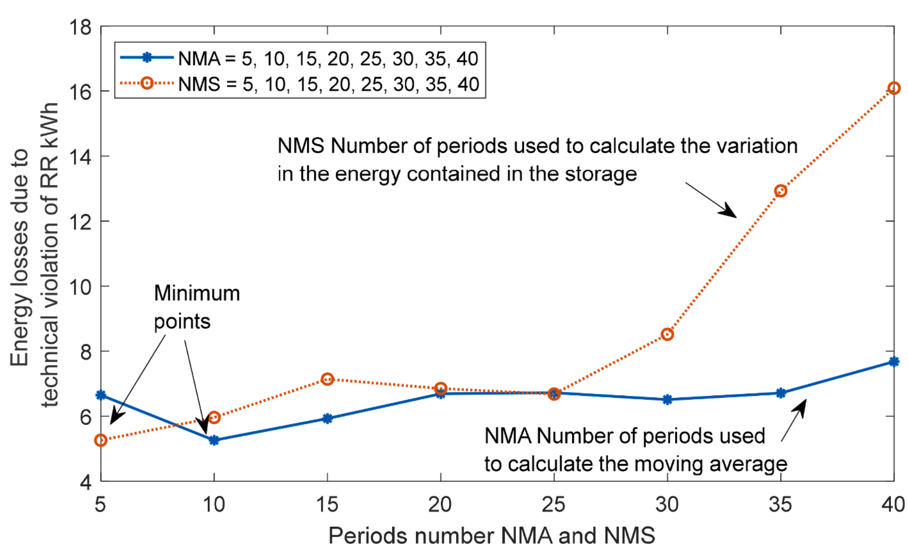

Fig. 17. Sensitivity analysis for NMS and NMS prediction values (PV = 15 kWp and SC = 400 Wh).

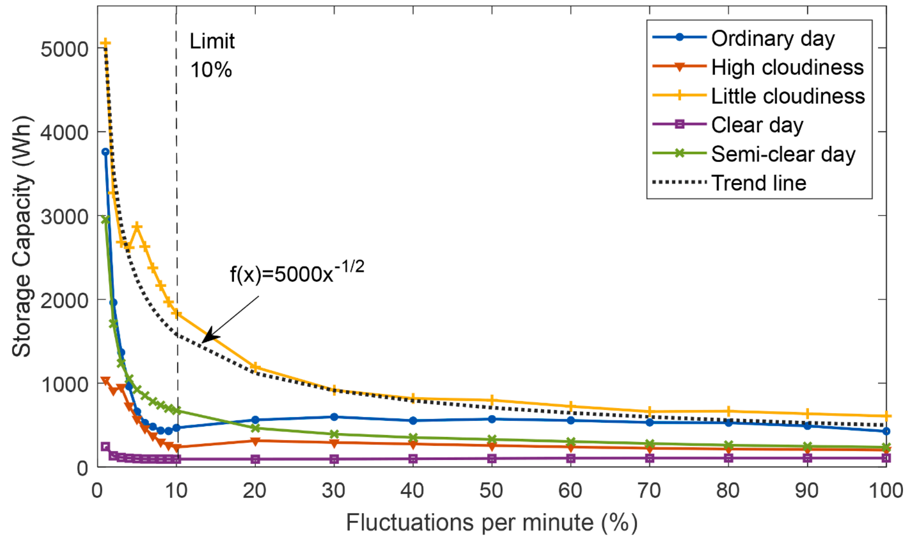

Fig. 18. Sensitivity analysis regarding the energy storage capacity and percentage reduction of PV fluctuation for different sky conditions.

Table 5
Results of the economic analysis of the new proposed method.

Item	Day	Cumulative annual occurrence frequency (day)	Energy PV Power (kWh/day)	Storage capacity (Wh/day)	Cost (USD)	Relative Additional Cost (RAC) (%)
1	Ordinary day	170	46.85	450	12,375.00	82.50%
2	High cloudiness	50	27.40	220	6050.00	40.33%
3	Little cloudiness	55	66.21	1860	51,150.00	341.0%
4	Clear day	35	90.78	64	1760.00	11.76%
5	Semi-clear day	55	62.81	620	17,050.00	113.67%

clear day = (80–100) kWh.

It is evident that the days with the highest cumulative annual occurrence frequency are the "ordinary days" with 170. Therefore, the SC capacity at 450 Wh, the total cost of SC is USD 12,375 (82.50% of the PV cost). Table 4 shows the results for different days of the year, in some cases the Relative Additional Cost (RAC) reaches values of 341% and in other cases of 11.76% depending on weather conditions.

7. Conclusions

This paper presents a novel power smoothing method using supercapacitors for grid-connected photovoltaic systems. The main novelty of the new method is based on two stages, prediction and correction. During the prediction stage, an application model of the simple k-means algorithm based on unsupervised machine learning is developed, with the aim of reducing big data by selecting representative data of the photovoltaic power fluctuations and charge/discharge cycles of the supercapacitor over a long time period (one year) using WEKA and MATLAB software. Then, for the correction stage, the ramp rate algorithms and combines the photovoltaic prediction, the supercapacitors duty cycles and their energy variation contained in storage has been used to generate the reference signals. To validate the new method, exhaustive laboratory experiments have been done using the ramp rate of 10%/min of PV capacity as the maximum allowed. The results are summarized below:

Firstly, the response of the power smoothing of the new method has been compared with respect to the moving average and ramp rate algorithms. It is evident that the new predictor-corrector method manages to reduce the unused power, this result is related to the control of the power smoothing band in the state of charge of the supercapacitor. In certain cases, it is not necessary to use a supercapacitor due to the resolution of the algorithm and the ability to detect short-term PV power. In such cases, according to the proposed predictor-corrector method, by considering the state of charge as a controllable variable it is possible to keep the power smoothing band within the assigned limits.

The proposed cluster technique was able to classify fluctuation values and relate to supercapacitor charge/discharge cycles from a one-year database. These results optimize the computational effort and could serve as a basis for dimensioning studies of large energy storage systems with limitations in charge and discharge cycles. In this context, the cluster analysis shows that the number of rising and falling PV power peaks over the course of a year is different, i.e., a difference of 323/month and 10.76/day. This indicates the importance of state of charge controlling of the supercapacitor.

The predictive-corrective characteristic of the new method we are proposing avoids the unnecessary use of supercapacitors in certain conditions by establishing the output power of a supercapacitor as the reference signal. Extensive experiments under different sky conditions show that the energy losses with P-C are lower with respect to moving average and ramp rate respectively.

The sensitivity analyses under different number of periods used to calculate the moving average (NMA) and number of periods used to calculate the variation of the energy contained in the storage (NMS) indices show that the classification of sky conditions establishes the minimum value of energy that can be defined with NMA = 10 and NMS = 5. It is evident that the energy change for the storage capacity (Wh) of the SC obtains its minimum value in the range of [0–5] for the power correction intensity modulation coefficient (CC), which indicates that it is feasible to define a short period.

Finally, the result of the sizing optimization shows that a SC system of 0.45 kWh capacity with respect to the PV system 15 kW is enough to smooth power peaks with ramp rates of ±10%/min with a relative additional cost of 82.5% of PV.

Declaration of Competing Interest

The authors declare that they have no known competing financial interests or personal relationships that could have appeared to influence the work reported in this paper.

Data availability

Data will be made available on request.

Acknowledgements

The first author is grateful for a Doctoral Training Program in the area of Engineering and Technical Sciences (UMA, Spain; UTI, UTM, UTN, Ecuador) of Asociación Universitaria Iberoamericana de Postgrado (AUIP).

The author (Paul Arévalo) thanks the "Call for Grants for the Requalification of the Spanish University System for 2021-2023, Margarita Salas Grants for the training of young doctors awarded by the Ministry of Universities and financed by the European Union –Next Generation EU".

Finally, the authors thank Universidad de Cuenca for easing access to the facilities of the Microgrid Laboratory of the Centro Científico Tecnológico y de Investigación Balzay (CCTI-B), for allowing the use of its equipment, and for authorizing its staff the provision of technical support necessary to carry out the experiments described in this article.

References

[1] Rahmann C, Vittal V, Ascui J, Haas J. Mitigation control against partial shading effects in large-scale PV power plants. IEEE Trans Sustain Energy 2016;7:173–80. https://doi.org/10.1109/TSTE.2015.2484261.

[2] Karimi M, Mokhlis H, Naidu K, Uddin S, Bakar AHA. Photovoltaic penetration issues and impacts in distribution network – A review. Renew Sustain Energy Rev 2016;53:594–605. https://doi.org/10.1016/J.RSER.2015.08.042.

[3] Shivashankar S, Mekhilef S, Mokhlis H, Karimi M. Mitigating methods of power fluctuation of photovoltaic (PV) sources – A review. Renew Sustain Energy Rev 2016;59:1170–84. https://doi.org/10.1016/J.RSER.2016.01.059.

[4] Kim HS, Okada N, Takigawa K. Advanced grid connected PV system with functions to suppress disturbance by PV output variation and customer load change. Sol Energy Mater Sol Cells 2001;67:559–69. https://doi.org/10.1016/S0927-0248(00)00328-7.

[5] Guo T, Liu Y, Zhao J, Zhu Y, Liu J. A dynamic wavelet-based robust wind power smoothing approach using hybrid energy storage system. Int J Electr Power Energy Syst 2020:116. https://doi.org/10.1016/J.IJEPES.2019.105579.

[6] Martins J, Spataru S, Sera D, Stroe DI, Lashab A. Comparative study of ramp-rate control algorithms for PV with energy storage systems. Energies 2019;12:1342. https://doi.org/10.3390/EN12071342.

[7] Akagi S, Yoshizawa S, Ito M, Fujimoto Y, Miyazaki T, Hayashi Y, et al. Multipurpose control and planning method for battery energy storage systems in distribution network with photovoltaic plant. Int J Electr Power Energy Syst 2020:116. https://doi.org/10.1016/J.IJEPES.2019.105485.

[8] Kryonidis GC, Nousdilis AI, Pippi KD, Papadopoulos TA. Impact of power smoothing techniques on the long-term performance of battery energy storage systems. In: 2021 56th Int. Univ. Power Eng. Conf. Powering Net Zero Emiss. UPEC 2021 - Proc. Institute of Electrical and Electronics Engineers Inc; 2021. https://doi.org/10.1109/UPEC50034.2021.9548172.

[9] Cao Y, Wu Q, Zhang H, Li C. Optimal sizing of hybrid energy storage system considering power smoothing and transient frequency regulation. Int J Electr Power Energy Syst 2022:142. https://doi.org/10.1016/J.IJEPES.2022.108227.

[10] Alam MJE, Muttaqi KM, Sutanto D. A novel approach for ramp-rate control of solar PV using energy storage to mitigate output fluctuations caused by cloud passing. IEEE Trans Energy Convers 2014;29:507–18. https://doi.org/10.1109/TEC.2014.2304951.

[11] Hurtt J, Baker K. Sensitivity analysis of photovoltaic system design parameters to passively mitigate ramp rates. IEEE J Photovoltaics 2021;11:545–51. https://doi.org/10.1109/JPHOTOV.2020.3045679.

[12] Kini R, Raker D, Stuart T, Ellingson R, Heben M, Khanna R. Mitigation of PV variability using adaptive moving average control. IEEE Trans Sustain Energy 2020;11:2252–62. https://doi.org/10.1109/TSTE.2019.2953643.

[13] Zhou H, Bhattacharya T, Tran D, Siew TST, Khambadkone AM. Composite energy storage system involving battery and ultracapacitor with dynamic energy management in microgrid applications. IEEE Trans Power Electron 2011;26:923–30. https://doi.org/10.1109/TPEL.2010.2095040.

[14] Zhang D, Chen Y, Wang L, Liu J, Yuan R, Wu J, et al. Control strategy and optimal configuration of energy storage system for smoothing short-term fluctuation of PV power. Sustain Energy Technol Assess 2021;45:101166. https://doi.org/10.1016/J.SETA.2021.101166.

[15] Das BK, Hasan M, Das P. Impact of storage technologies, temporal resolution, and PV tracking on stand-alone hybrid renewable energy for an Australian remote area application. Renew Energy 2021;173:362–80. https://doi.org/10.1016/J.RENENE.2021.03.131.

[16] Patel S, Ahmed M, Kamalasadan S. A novel energy storage-based net-load smoothing and shifting architecture for high amount of photovoltaics integrated power distribution system. IEEE Trans Ind Appl 2020;56:3090–9. https://doi.org/10.1109/TIA.2020.2970380.

[17] Siratarnsophon P, Lao KW, Rosewater D, Santoso S. A voltage smoothing algorithm using energy storage PQ control in PV-integrated power grid. IEEE Trans Power Deliv 2019;34:2248–50. https://doi.org/10.1109/TPWRD.2019.2892611.

[18] Wang G, Ciobotaru M, Agelidis VG. Power smoothing of large solar PV plant using hybrid energy storage. IEEE Trans Sustain Energy 2014;5:834–42. https://doi.org/10.1109/TSTE.2014.2305433.

[19] Gkavanoudis SI, Demoulias CS. A combined fault ride-through and power smoothing control method for full-converter wind turbines employing Supercapacitor Energy Storage System. Electr Pow Syst Res 2014;106:62–72. https://doi.org/10.1016/J.EPSR.2013.08.007.

[20] Marcos J, de La Parra I, García M, Marroyo L. Control strategies to smooth short-term power fluctuations in large photovoltaic plants using battery storage systems. Energies 2014;7:6593–619.

[21] Premadasa PND, Chandima DP. An innovative approach of optimizing size and cost of hybrid energy storage system with state of charge regulation for stand-alone direct current microgrids. J Energy Stor 2020;32:101703. https://doi.org/10.1016/J.EST.2020.101703.

[22] Malamaki KND, Casado-Machado F, Barragan-Villarejo M, Gross AM, Kryonidis GC, Martinez-Ramos JL, et al. Ramp-rate limitation control of distributed renewable energy sources via supercapacitors. IEEE Trans Ind Appl 2022. https://doi.org/10.1109/TIA.2022.3195975.

[23] Sukumar S, Mokhlis H, Mekhilef S, Karimi M, Raza S. Ramp-rate control approach based on dynamic smoothing parameter to mitigate solar PV output fluctuations. Int J Electr Power Energy Syst 2018;96:296–305. https://doi.org/10.1016/J.IJEPES.2017.10.015.

[24] Kumar DS, Maharjan S, Albert Srinivasan D. Ramp-rate limiting strategies to alleviate the impact of PV power ramping on voltage fluctuations using energy storage systems. Sol Energy 2022;234:377–86. https://doi.org/10.1016/J.SOLENER.2022.01.059.

[25] Lappalainen K, Valkealahti S. Sizing of energy storage systems for ramp rate control of photovoltaic strings. Renew Energy 2022;196:1366–75. https://doi.org/10.1016/J.RENENE.2022.07.069.

[26] Chong LW, Wong YW, Rajkumar RK, Isa D. An optimal control strategy for standalone PV system with Battery-Supercapacitor Hybrid Energy Storage System. J Power Sources 2016;331:553–65. https://doi.org/10.1016/J.JPOWSOUR.2016.09.061.

[27] Malamaki KND, Kryonidis GC, Demoulias CS. Comparative evaluation of ramp-rate limitation control strategies employing supercapacitors. In: MELECON 2022 - IEEE Mediterr. Electrotech. Conf. Proc., Institute of Electrical and Electronics Engineers Inc.; 2022. p. 207–12. https://doi.org/10.1109/MELECON53508.2022.9842921.

[28] Gevorgian V, Baggu M, Ton D. Interconnection requirements for renewable generation and energy storage in island systems: Puerto Rico example. In: 4th Int. Hybrid Power Syst. Work., Crete, Grece; 2019.

[29] Sukumar S, Marsadek M, Agileswari KR, Mokhlis H. Ramp-rate control smoothing methods to control output power fluctuations from solar photovoltaic (PV) sources—A review. J Energy Stor 2018;20:218–29. https://doi.org/10.1016/J.EST.2018.09.013.

[30] Kakimoto N, Satoh H, Takayama S, Nakamura K. Ramp-rate control of photovoltaic generator with electric double-layer capacitor. IEEE Trans Energy Convers 2009;24:465–73. https://doi.org/10.1109/TEC.2008.2001580.

[31] Kumar MR, Ghosh S, Das S. Charge-discharge energy efficiency analysis of ultracapacitor with fractional-order dynamics using hybrid optimization and its experimental validation. AEU - Int J Electron Commun 2017;78:274–80. https://doi.org/10.1016/J.AEUE.2017.05.011.

[32] Rana MM, Uddin M, Sarkar MR, Shafiullah GM, Mo H, Atef M. A review on hybrid photovoltaic – Battery energy storage system: Current status, challenges, and future directions. J Energy Stor 2022;51:104597. https://doi.org/10.1016/J.EST.2022.104597.

[33] Gevorgian V, Booth S. Review of PREPA Technical Requirements for Interconnecting Wind and Solar Generation. 2013.

[34] Davies DL, Bouldin DW. A Cluster Separation Measure. IEEE Trans Pattern Anal Mach Intell 1979. https://doi.org/10.1109/TPAMI.1979.4766909. PAMI-1:224–7.

[35] Espinoza JL, Gonzalez LG, Sempertegui R. Micro grid laboratory as a tool for research on non-conventional energy sources in Ecuador. In: 2017 IEEE Int. Autumn Meet. Power, Electron. Comput. ROPEC 2017. vol. 2018. Janua, Institute of Electrical and Electronics Engineers Inc.; 2018. p. 1–7. https://doi.org/10.1109/ROPEC.2017.8261615.

[36] Atersa | Atersa Grupo Elecnor n.d. https://www.atersa.com/ (accessed January 8, 2023).

[37] Maxwell Technologies - Welcome to a Power Revolution n.d. https://maxwell.com/ (accessed January 8, 2023).

[38] de la Parra I, Marcos J, García M, Marroyo L. Control strategies to use the minimum energy storage requirement for PV power ramp-rate control. Sol Energy 2015;111:332–43. https://doi.org/10.1016/J.SOLENER.2014.10.038.